Behavioral individuality is a consequence of experience, genetics and learning

Riddha Manna[1], Johanni Brea[1,2], Gonçalo Vasconcelos Braga[1], Alireza Modirshanechi[1,2], Ivan Tomić[3], and Ana Marija Jakšić[1*]

[1]École Polytechnique Fédérale de Lausanne, School of Life Sciences, Brain Mind Institute, Lausanne, 1015, Switzerland
[2]École Polytechnique Fédérale de Lausanne, School of Computer and Communication Sciences, Lausanne, 1015, Switzerland
[3]École Polytechnique Fédérale de Lausanne, School of Engineering, Discovery Learning Laboratories, Lausanne, 1015, Switzerland
[*]ana.jaksic@epfl.ch

ABSTRACT

Genetic determinism of behavior supposes that behaviors are fundamentally defined by genetics[1–3]. However, behaviors are also modified by development[4], environment[5,6], and learning[7–9]. It is assumed that if we could control all of these factors, behavior would be genetically predictable. These factors, however, cannot be controlled in humans, and have been impervious to dissection and joint control even in animal models[10–17]. How genotype[13] and life experience[16] interact to shape individual behavior through learning[17] has been lacking experimental evidence, and thus remains only hypothesized[8]. Here, we design an experimental platform which allowed for multi-generational control over genetics, development, environment and experience. We measure learning-dependent individuality and its sources across thousands of genetically diverse *Drosophila*. We show that genetics plays an essential role in shaping the distributions of individual behaviors. Further, we find that genotype-specific bias shapes individual experience, which in concert with learning, causes dynamic evolution and diversification of individual behavior, even in a uniform environment. We experimentally derive that individual past life experience, genetics, and learning, in this order, shape the momentary individual expression of behavior. Finally, while association studies frequently report the opposite, we show experimentally that life experience severely diminishes the predictive power of genetics for individual learning-dependent behavior.

Introduction

Although genes have a strong impact on behavior[1,18–20], even identical twins with the same developmental history, anatomy, and physiology eventually diverge behaviorally into two distinct individuals[4,21,22]. Initially, this divergence is driven by two opposing forces: genetic determinism and molecular stochasticity[1,23,24]. Later, behavior can also change due to learning and memory[8,16,18,25–27]. The relative importance of these forces for defining individual behavior and cognitive performance has remained debated[1,28]. This is because the ability to learn and remember is also known to vary across environments[29], genotypes[30,31], individuals[8,9,32–34] and even maternal status[35–37]. These factors also interact with each other and are thus challenging to control in concert, so the relative impact of different sources of individuality is difficult to determine (Figure 1A). In particular, studying individuality of learning-dependent behaviors requires a high level of trans-generational experimental control over individual genetic and environmental conditions across many individuals[8,38–40]. In humans, this is not ethically possible - lifelong experiences of any two individuals are never identical[22] and their genetic background is usually confounded with social, cultural and economic life history[21]. Fortunately, when we study behavior in experimentally accessible organisms, one can design experiments that approach extreme experiential uniformity across individuals and genotypes, allowing us to disentangle the sources of variability[4,12–15,41,42]. To account for the omnipresent environmental stochasticity, behavior of a genotype is usually measured across multiple isogenic groups or individuals, while an individual's behavior is measured across multiple time-points or tasks[13,17,18]. The consistency in behavior is then used to discriminate between noise and the behavioral identity of an individual or a genotype. However, this approach to studying individuality is limited to behaviors that are stable within individuals and over time[4,11–13,15,25,34]. Learning from experience, however, induces temporal changes in individual behavior[8,26]. Because of this, investigating the genetic basis of individuality in learning-dependent settings additionally requires experiential uniformity across individuals[16,34]. This is challenging but can be achieved through extensive parallelization of individual, time-resolved behavioral tests in diverse and replicated isogenic populations, where experience can be quantified

and aligned across individuals. Each individual can then be considered a repeated measurement of a genotype in the same environment, at the same time and at nearly the same space, closely approaching experiential uniformity. Unfortunately, such multiplexed assays for learning-dependent behaviors are lacking, even for animal models where all sources of individuality can be tightly and jointly controlled. Consequently, there is no clear experimental evidence supporting the dominance of one source of individuality over the others. Specifically, how genotype, experience, and learning interplay to shape behavioral individuality has not been examined in genetically diverse populations under required concerted developmental, environmental, experiential and genetic control. Nevertheless, due to their scientific as well as societal significance, the association and the relative impact of genetics and learning on behavior has been studied and discussed (often with great conviction)[1,28,43]. Yet, how individual learning-dependent behavior emerges from genetics or life circumstance remains unknown. Here, we tackle this fundamental question in a well-established animal genetics model, the vinegar fly (*Drosophila melanogaster*). Flies express complex behaviors that are essential for cognition, including learning and memory-dependent behavior[44–47]. In addition, their genetic diversity, the relative ease of controlling their life history and tracking their behavior[48,49] make flies an ideal model to study the relative contributions of genetics and learning on individuality. Learning in flies is measured with conditioning assays[44,50]. However, existing assays are largely non-parallelized, low in sample- or test- throughput and, due to their complexity, often need to relax constraints on environmental uniformity[4,31,34,51–58]. Here, we first solve the technological challenge to study the genetics of individuality in a learning-dependent task. We then use our method to dissect the sources of emergent behavioral individuality in learning-dependent behaviors across 90 diverse genetic backgrounds. By analyzing and modeling the time-resolved individual experience of over 6000 individual flies making over half a million decisions, we partition the contributions of genetics, learning and life experience to behavioral individuality.

Results

Behavioral individuality is genetically variable

We designed a platform that implements operant conditioning assays parallelized across 64 freely behaving individual *Drosophila melanogaster* (Figure 1B). The system takes input from real-time video tracking of individuals (Video S1). This is then used for closed-loop coupling of visual stimuli and delivery of a mild foot shock to individual flies upon an undesired behavior (Figure 1C-D, S1A). Implemented operant conditioning paradigms are based on avoidance learning in a Y-shaped arena ("Y-maze"; see Methods). The conditioned task was to spend less time in an arm ("place learning" paradigm) or on a color (green or blue; "color learning" paradigm) that was associated with the shock (Figure 1C, S1A; see Methods). This was measured as the proportion of the total time spent in the shocked arm ($T_{shocked}$, task performance, Figure 1E). When no shock was applied throughout the assay (control group), and assuming no innate biases, flies were expected to spend a third, and a half of their time in each arm and color, respectively (Figure 1D-E). The difference between mean control and conditioned $T_{shocked}$ of a genotype (*"relative task performance"*) emulated the traditionally used group-average measures of task performance[19] (Figure 1F, Figure S1C). We also confirmed that the platform robustly and successfully captured classical genetic deficits in core cognitive behaviors, such as learning, memory and visual perception[19,59,60] (Figure 1E-F, Figure S1B-E, S2A).

We used the platform to further explore the dynamics of individual behaviors in wild-type and laboratory genotypes (Figure 2A, S2A-B). We measured the genetic effects on individual learning-dependent behavior in 5632 flies derived from 88 genetically distinct and isogenic wild-type genotypes[48] (Figure 1F, 2A, S3A). To remove the influence of the environment on variation in behavior, we first ensured strict multi-generational control over life-history. All flies were reared uniformly and assayed at the same age, the same time of the day, and in the same environment (Table S1). Two independently reared populations of individuals of the same genotype (replicates 1 and 2) were measured in parallel and used to estimate the extent of any remaining systematic experimental variation which the flies may have experienced but which we could not control (Figure 2B, 2F, S3B-I). We recorded over 1 million video frames to extract almost half a million individual decisions (i.e., switches from one arm in the Y-maze to another arm; N = 497450), task performance, and a range of task-relevant behaviors.

Task performance in the presence of shock (conditioned treatment) and spontaneous behavior in the absence of shock (control treatment) were tested in the visual green place learning paradigm parallelized between adult individual flies (88 genotypes, N = 5238 flies after filtering; see Methods). On average, $T_{shocked}$ for conditioned flies was significantly lower than for the control flies (23.3% vs. 29.9%, N = 2611 and N = 2627, respectively; T-test $p < 2.2e^{-16}$; Figure 2A, 2D, S4A). The majority of genotypes (77 out of 88, 87.5%) showed a positive (mean > 0) relative task performance (Figure 1F), which varied significantly between genotypes (ANOVA $p < 2.2e^{-16}$, Sum Sq. = 3.143; Figure 1F, Table S2). This was consistent when shocked and neutral colors were swapped (Figure S1C, Table S3). We found no difference between males and females (ANOVA p = 0.537, Sum Sq. = 0.004, Table S2).

There was a marked time-dependent and significant decrease in $T_{shocked}$ in the conditioned flies (Figure S4A, S4F, S4K). On average, other spontaneous individual behaviors, such as handedness, velocity, color preference and relative difference in velocity between the shocked and non-shocked arms of the Y-maze, changed upon conditioning (Figure S4B-E). Curiously, they also changed significantly and consistently over time (Figure S4G-J). This phenomenon was more dramatic in the conditioned

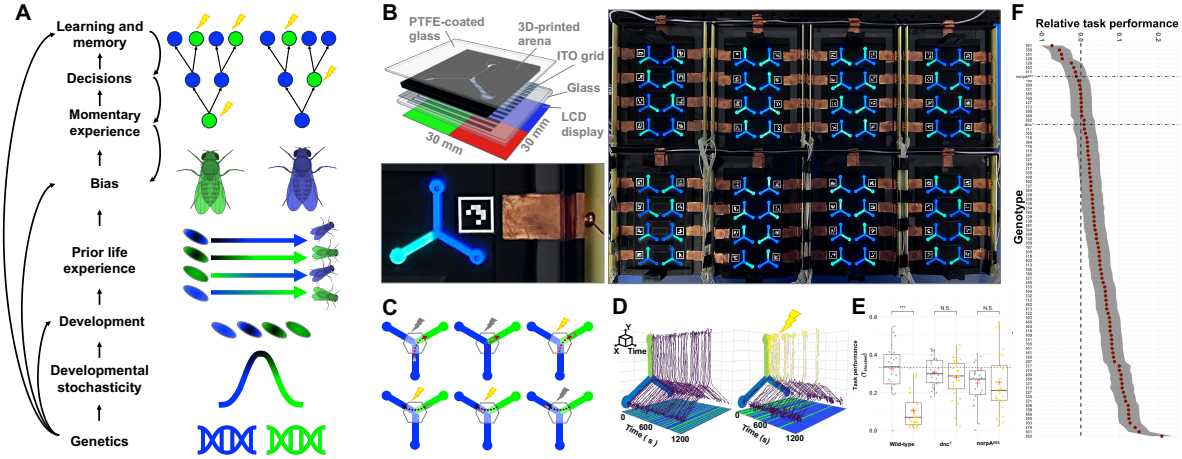

Figure 1. Capturing individual learning-dependent behavior across genotypes. A) Sources of individual behavior. In a single environment, genetic, stochastic, and experiential sources of individuality interact with each other to produce behavior such as color bias. Past, individual experiences can result in behavioral biases that guide initial decisions. In the presence of valent experience, learning and memory from momentary experience can change the future bias and influence future decisions in a loop. Variation in genotype can influence any source of individuality, directly or indirectly. Its effect is thus confounded with experience and learning. **B)** Schematic of a Y-maze design (top left panel), top-down view of the 64-maze multiplexed platform with randomized visual stimuli (right), and a close-up photograph of a single Y-maze arena (bottom left). **C)** Schematic of a shock delivery and shock removal timing upon a discrete decision in a visual place learning task: shocks are applied at 30V DC and (on average) 7.8 mA from the moment a fly has fully entered the shock arm (top right) until it has fully entered a new arm (bottom right). **D)** Representative tracks of two flies traversing a Y-maze in the presence (right) or absence (left) of conditioning. Lines on the bottom represent color occupancy. **E)** Task performance in green place learning task (green arm is shocked) of a wild-type genotype compared to the memory and learning mutant (dnc^1) and the visually impaired mutant ($norpA^{EE5}$). Measurements of individual control (grey) and conditioned (yellow) flies are shown as points. Boxes indicate the upper and lower quartiles, mean and medians are represented as bar and red plus, respectively. **F)** Relative task performance in place learning task across 90 genotypes uncovers genetic variability. Grey shading indicates standard error. Vertical line points to no change in performance upon conditioning (0) and horizontal lines indicate relative task performance for memory- and vision-deficient genotypes (dnc^1 and $norpA^{EE5}$).

group, indicating that even apparently stable behaviors can change within a 20-minute conditioning assay. Accordingly, we concluded that repeated measurements of a single individual over time cannot be used to disentangle experimental noise from learning-dependent individuality in a straightforward way.

Despite the parallelized measurements and strict multi-generational, replicated control over individuals' environment and genetics (Table S1, Figure S3B-I, Table S4), we found non-negligible behavior variability within groups of genetically identical individuals (Figure 2A, S3A). Curiously, we found that not only the means (Figure 2D), but also the shapes of the distributions of individual behaviors varied reproducibly between genotypes, particularly in the conditioned group (Figure 2A-B, S3B). We asked what is the source of this expressed individuality, and whether its nature is stochastic or deterministic.

Individuality of learning-dependent behavior is not random

In the absence of shock, the individuals from most genotypes visited different parts of the Y-maze seemingly stochastically, at a near-chance level (Figure 2A, S3A). In line with the expected effects of developmental stochasticity[25,61,62], individual task performance ($T_{shocked}$) of the control group generally assumed a normal distribution within a genotype (Figure 2A-B, S3A, S5). Curiously, this was not the case in the conditioned group. Despite the shared developmental history and life history with the control flies, in the conditioned flies, the distributions of individual task performances within a genotype assumed a variety of shapes that appeared non-Gaussian and multi-modal (Figure 2A-B, S3A, S5). These patterns were reproducible across independently raised replicates (Exact general independence test, $p > 0.05$ for 83 out of 88 genotypes; see Methods; Figure 2B, S3B). The replication of different genotype-specific distributions of $T_{shocked}$ demonstrated that the extent of expressed individuality is in some way genetically controlled. Genotype is known to influence developmental stochasticity and can therefore affect the variance of any behavioral measure[18]. Different environmental conditions experienced by individuals (or

inconsistent control over them) can also affect within-genotype distribution of behaviors (both mean and variance)[63]. This can be a result of either the direct effect of a single environment on developmental stochasticity of a genotype, or the interaction of the genotype with multiple, individually experienced environments. Together, these processes could potentially cause various distributions of a phenotype within a genotype. To characterize and dissect the genetic contribution to the unusual display of individuality we observed, we could not use measures of variation such as variance, which is usually used to quantify variability in Gaussian distributions. Therefore, to describe the extent of individuality expressed within a genotype we use differential entropy (H), which captures the amount of information encoded in the probability distributions of individual behavior within a genotype that are not necessarily Gaussian (Methods). To quantify the difference in expressed individuality between two groups of flies, the Hellinger distance between the two probability distributions is calculated (Methods). We found that the entropy of the $T_{shocked}$ distribution was highly genotype-dependent (Resampling test, parametric $p < 2.2e^{-16}$ resampled $p = 1e^{-06}$, Figure S6A), and it correlated between tested environments (Pearson's product-moment correlation between $H_{control}$ and $H_{conditioned}$ $r = 0.232$, $p = 0.03$, n= 88 genotypes, Figure S6A). The difference in expressed individuality between the tested environments (conditioned and control) varied substantially between genotypes (Resampling test, parametric $p < 2.2e^{-16}$, resampled $p = 1e^{-06}$, Figure S6B). At the same time, the difference in expressed individuality within a genotype, between replicates was consistently low in both conditioned and control flies (Mean $Hellinger_{control} = 0.06$, Mean $Hellinger_{conditioned} = 0.05$, T-test $p = 0.256$, n = 88, Figure S6C), demonstrating that the life history was tightly controlled. Together, these results indicated that, to a great extent, the observed genotype-specific behavioral variability is sourced from mechanisms that are not entirely random, but are systematically shared between all flies of the same genotype, such as shared impact of genotype on developmental stochasticity or genotype's interaction with experimental stochasticity.

Although we found that the genotype-dependent entropy largely correlated between two tested environments (control and conditioned), the shapes of the distributions of individual task performance were markedly different in each environment as well as between genotypes (Figure 2A-B, S3A). This implied that the extent of individuality expressed within a genotype is not linearly translated from control to conditioned behavior. We reasoned there must be a source of individuality that cannot be segregated to usual effects of genotype on variability, such as its modulation of developmental stochasticity or its interaction with the shared environmental noise. This source of individuality cannot be attributed to common life history prior to the task. To capture sources of individuality that go beyond the usual effect of genotype or noise on the distribution of behaviors, we turned to measures that can quantify this hypothesized "residual", non-developmental source of individuality.

To do so, we introduce a measure of residual individuality (H_{resid}), calculated as Shannon entropy of a probability distribution after scaling the distribution within its own range to nullify the effect of the variance induced by life-history factors shared across all groups of flies, such as stochastic processes, genotype, environment and their interactions (Figure S7, Methods). We then use different measures of "shape divergence" (*shape Div*) which capture divergence in residual individuality. *Shape Div* is obtained by measuring the Kullback-Leibler divergence of two distributions, independently scaled within their own range (Methods). With this, we define the *environmental variability* (*EV*) as the divergence in the shape of the scaled distributions of $T_{shocked}$ of the conditioned flies from that of the control flies (Figure 2C, 2G; see Methods). This *shape Div* quantifies the relative entropy, or the change in expressed residual individuality (H_{resid}) of a genotype due to conditioning. Importantly, this measure is insensitive to the difference in mean behavior across individuals (Methods), or to the differing ranges of expressed behavior in the two treatments (control and conditioned). In the same way, the divergence of scaled distributions from one replicate to another reflects the change in residual individuality caused by systematic experimental noise distributed over individual flies during the behavior assay that is not caused by the genotype's interaction with the environment (*measurement variability*, *MV*, Figure 2F). Lastly, the divergence in residual individuality of one genotype from another captures the genetic contribution to the expressed residual individuality beyond the genotype's control over developmental noise or its interaction with the environment shared between genotypes prior to the behavior assay (*genetic variability*, *GV*, Figure 2E).

Environmental variability of $T_{shocked}$ (*EV*) was significantly variable across genotypes (Resampling test, parametric $p < 2.2e^{-16}$, resampled $p = 1e^{-06}$; Figure 2C), and evolved with every made decision (Figure 2G), yet we found no difference in *measurement variability* between conditioned and control groups ($MV_{control} = 2.08$, $MV_{conditioned} = 1.85$, T-test $p = 0.206$, n = 88, Figure 2F). This indicated that individual experiences before the behavior was measured were consistently distributed across individual, independently raised flies. It also suggested that the environment in which the behavior was measured (conditioned or control) induced the observed change in residual individuality. In a fixed, shared environment, genetics is expected to be the only deterministic variable that can shape individuality. In isogenic populations, the effect of genotype on individuality beyond its effect on phenotype variance should be absent. Yet, the shapes of the distributions of individual $T_{shocked}$ were significantly more divergent between genotypes in the conditioned group than in the control group ($GV_{control} = 0.70$, $GV_{conditioned} = 0.83$, T-test $p < 2.2e^{-16}$, n = 88 genotypes; Figure 2E).

This genotype-dependent control over the change in residual individuality upon conditioning was not specific to $T_{shocked}$. We found it in other behaviors as well, including the learning score, handedness, decision-making, velocity and relative velocity (Figure S3E-I, S8A).

Residual heterozygosity[48] could not explain the diversity in residual individuality (H_{resid}) observed in any behavior (Figure S9A). This was also reflected by the significant difference in *genetic variability* between treatments (Figure 2E, *GV* in Figure S8A) and by the divergence between conditioned and control groups (Figure 2C, *EV* in Figure S8A), where compared groups of flies were sourced randomly from the same genetic pool.

Interestingly, while the shapes of distributions of $T_{shocked}$ diverged between genotypes (*GV*) and between environments (*EV*), the mean residual individuality (H_{resid}) for task performance across genotypes was not different between conditioned and control flies (Control $T_{shocked}$ H_{resid} = 2.04, Conditioned $T_{shocked}$ H_{resid} = 2.02, T-test p = 0.321, n = 88 genotypes, Figure S8B). In other words, the amount of residual individuality was the same, but distributed differently, depending on the environment. This was the case for other behaviors as well, except for the proportion of correctly made decisions (*percent correct*), where residual individuality (H_{resid}) was higher in conditioned flies (Figure S8A), and for *velocity* (Figure S8A), where it was lower in the conditioned flies, compared to control. This result was another indication that the observed changes in residual individuality upon conditioning are not random and cannot be explained by shared developmental or experimental stochasticity. How can genetically uniform experimental populations raised and tested in parallel, uniform and replicated environments still express varying, genotype-dependent and non-stochastic individuality across behavioral paradigms?

Our results suggested that the residual individuality is shaped by a genotype-dependent, non-random process specific to conditioning. Because the conditioned flies' divergence in residual individuality from control flies increased during the assay and evolved continuously with each decision (Figure 2C, 2G), we wondered if the cumulative experience of conditioning, and genotype's response to it, is the culprit behind the genotype-specific expression of individuality.

Individuality is shaped continuously through learning from experience

The only discriminating state between the conditioned and the control groups was the presence of a shock as a stressful or valent experience (punishment). Accordingly, two potential hypotheses can explain the increased divergence in expressed residual individuality across genotypes observed only in the conditioned group: 1. Genotype-specific individuality in shock sensitivity or 2. Genotype-specific individuality in learning. The locomotor *shock response* (Methods) of individual flies was, as expected, higher in the presence of shock (mean *shock response*$_{control}$ = 0.294 mm/s, mean *shock response*$_{conditioned}$ = 0.451 mm/s, T-test $p < 2.2e^{-16}$, n = 5238, Figure S9B). However, individual (Figure S8C) or genotype-specific (Figure S9A) *velocity*, *relative velocity*, *percent correct decisions*, *handedness*, or *task performance* did not correlate with *shock response* in the conditioned group. On the other hand, *learning score* (LS; Methods) correlated negatively and significantly with *task performance* in the conditioned group across individuals (Pearson's product-moment correlation r = -0.201, $p < 2.2e^{-16}$, n = 2611, Figure S8C) and across genotypes (Pearson's product-moment correlation r = -0.399, $p = 1e^{-04}$, n = 88 genotypes; Figure S9A). Individual *learning score* also correlated with individual *relative velocity* and *velocity* (Figure S8C). Together, this provides evidence that learning, rather than shock-sensitivity, is entangled with the increased expression of residual individuality under conditioning. Interestingly, it also shows that individual learning is associated with other, usually presumed learning-independent behaviors, such as velocity. Individual learning must play a key role in shaping individual task performance in the presence of shock, possibly by individually optimizing expression of other behaviors to minimize punishment. On the other hand, genotype-specific mean task performance and mean learning scores also correlated significantly (Figure S9A). Yet, there was a lack of correlation between either genotype-specific mean learning score or its residual entropy with residual entropy of task performance. This indicated that genetically encoded learning ability cannot explain genotype-specific residual individuality in task performance (Figure S9A).

Under the assumption of fixed environment and experience across genotypes and individuals, neither the stochastic processes, individual learning ability nor genetic background could independently provide a complete and satisfactory explanation for the observed residual individuality expressed upon conditioning. This led us to consider the possibility that we underestimated the impact of individual, momentary experience on behavior within a controlled experimental setting, or that we wrongly assumed that the uncontrolled effects of the environment during the task would be randomly distributed across individuals.

Despite the efforts to perfectly control and parallelize experienced environments across every individual, in practice, perfect control over biological, freely behaving agents, is rarely achievable. Experience of freely behaving individuals depends on their individual decisions (Figure 1A), which are practically intractable in a natural environment. However, the design of the Y-maze arena minimizes the diversity of unique experiences and decisions a fly can make, and allows us to enumerate them (Figure 3B). In particular, we could track how individual behaviors evolved from individual experiences resulting from a fly making decisions while traversing the maze (Figure 3A-C). By aligning individual experiences across many, behaviorally diverse individuals, we could ask how do momentary experiences impact the emergence of individual behavior. We found that the strategy of a fly exploring the Y-maze initially conformed to individual- and genotype-specific color biases, reflected in their positions in the maze at the start of a learning sequence (Figure S10A-B). Curiously, this genotype-specific bias created a slight variation in the distribution of the very first learning experience across individuals, namely the starting color and the associated presence of a shock. We had initially overlooked the importance of this experiential variation, as it represented

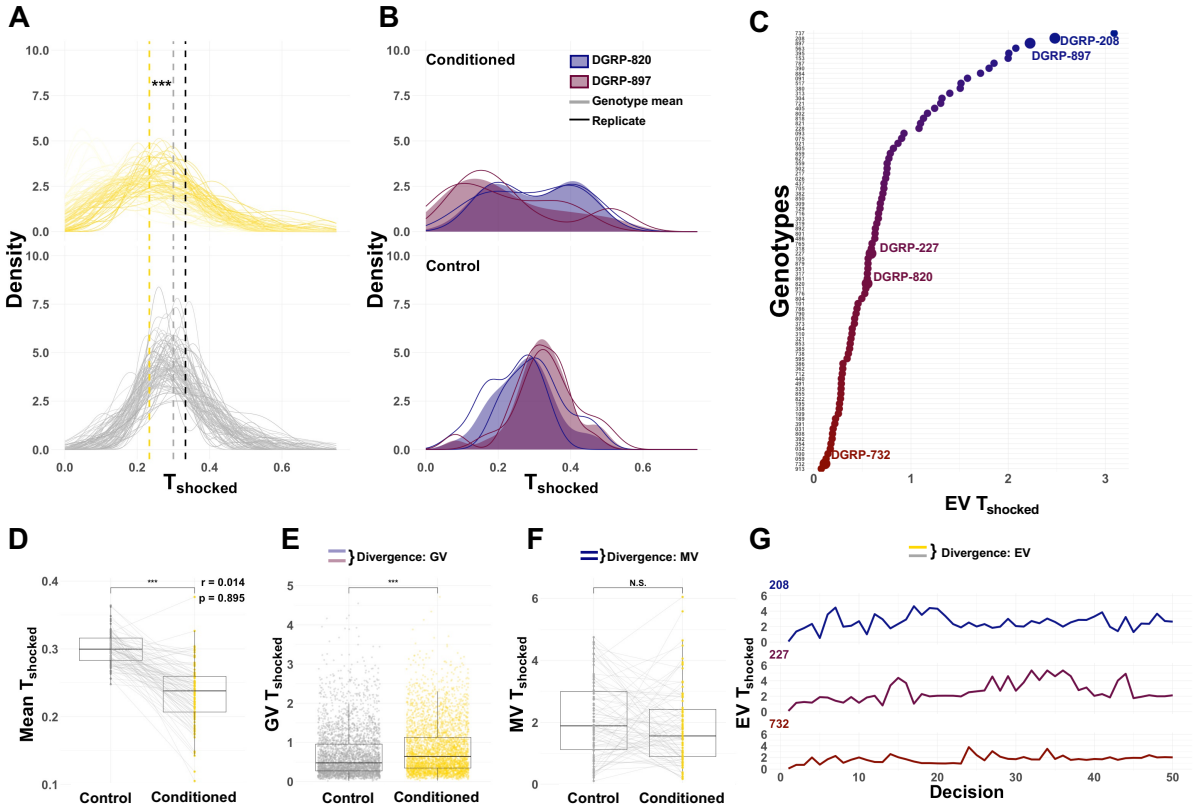

Figure 2. Residual individuality in task performance is not random. **A)** Distributions of individual task performance for each of the 88 wild-type genotypes in conditioned (yellow) and control (gray) task performance. Vertical lines show mean task performance for conditioned and control flies (yellow and gray), and chance expectation of $T_{shocked}$ at 1/3 (black). **B)** Genotype-specific extent of individuality is replicable and dependent on conditioning. An example of individual $T_{shocked}$ distributions in two genotypes (shaded red and blue) is shown. When visualized as independent distributions (shown as lines), replicates exhibit consistent distributions of individual $T_{shocked}$ within a genotype, despite being raised independently. Unlike the control (lower panel), the conditioned flies (upper panel) tend to assume non-Gaussian distributions of $T_{shocked}$. **C)** The change in residual individuality (comparison of shapes of same-colored distributions in B, and equivalent comparison across other genotypes) of $T_{shocked}$ upon conditioning compared to control is genotype-specific. **D)** Mean task performance across genotypes in conditioned flies (yellow) is significantly different from task performance in control flies (gray). Light-gray lines connect the same genotype's value across the two treatments. Inset text shows correlation for mean $T_{shocked}$ between two treatments and the associated p-value. **E)** Difference in expressed residual individuality between genotypes is significantly higher in conditioned (yellow) than in control treatment (gray). Each point represents *shape Div* of individual task performance distributions between two genotypes (*GV*). **F)** Extent of expressed residual individuality in task performance is similar between replicates, pointing away from systematic experimental variability as the source of change in residual individuality. Each point represents *shape Div* between two replicates of a genotype (*MV*). **G)** Divergence in expressed residual individuality of conditioned flies from control flies (*EV*) evolves with every decision and increases over time.

a seemingly negligible single-decision difference. However, we found that the way a fly experiences punishment the first time had the potential to cumulatively change the evolution of its future decisions (Figure 3A, 3C, 3E). On the other hand, in the absence of the valent experience (in control flies), the first experience did not have an effect on the evolution of the task outcome of an individual, but it reflected only the individual's or genotype's bias. Specifically, while the task performance was (unsurprisingly) correlated with color bias (Figure S8C), the *change* in task performance was more sensitive to starting position in the conditioned flies than in the control flies. This correlated with the flies' individual learning score (Figure 3D) but not with their color bias (Figure S10C). The effect of the initial position in conditioned flies had an unexpectedly long-lasting effect on the temporal evolution of task performance (Figure 3A, 3C, 3E, S10D). The convergence of task performance of individuals starting at different positions yet sharing a color bias lagged substantially, even for flies that shared a high learning score or favorable color bias (Figure 3A, S10D). Moreover, the divergence in residual individuality between flies starting at different positions was persistently high for good learners, especially those expressing an unfavorable initial color bias. This indicated that an interplay between bias and learning exacerbates residual individuality (Figure 3E). We reasoned that the effect of the starting position on divergent task performance stems from the clash between developmentally determined color bias and individual learning at the beginning of the learning task, when the association of the color with punishment is just becoming established. In support of this hypothesis, an individual's learning ability was a progressively more salient predictor of conditioned task performance over time (Figure S10E), while the initial color bias was predictive of the fly's performance only at the beginning of the task, or in the absence of conditioning (Figure S10F). We could also directly observe the clash between learning and bias as it played out in the initial decision-making (Figure 3C). This was most apparent in the persistent color switching behavior that was most prominent in flies with high learning score and unfavorable bias, and for which the resolution of the clash occurred much later (Figure 3C, 3E). Together, these dynamics illustrate how genotype, experience and learning influence individuality. First, the genotype-specific color bias creates a genotype-specific divergence in initial experience across individuals. Then, due to the introduction of punishment (a valent experience), the individual biases change in a manner that depends on the individual choices. Finally, as each individual's bias changes, so does each individual's probability of the next decision. Thereby, an individual learning-experience event closes and advances to its next iteration (Figure 1A).

In summary, genetic and individual biases acquired during development or life can define the probability of a distinct experience at both the individual and the genotype level. As the flies independently and individually learn to abandon unfavorable biases or lean into favorable ones, they influence how they choose and experience their own next decisions. This dynamic process produces an initially genetically seeded experience (Figure S10B) that instigates individually evolving (Figure 2G, 3A, 3C, 3E) behavioral flux resulting in the emergence of experience-based individuality. In environments more realistic than the Y-maze, this string of experiences is bound to be more diverse and cause intractable divergence of individual behaviors.

Experience-based individuality dismantles genetic predictability of behavior

In natural populations, sources of variability in life experience are intractable. While we do not track individual flies throughout their entire lives, the design of our experiment allows us to dissect the effects of life experience before the task from the effects of momentary experience during the task. We therefore asked how extensive is the effect of the entire life's experience on individual, momentary behavior, compared to the effect of genetics or learning during the task? To quantify the relative contributions of different sources of individuality, we turned to modeling of observed behaviors. We tested how well our models capture and represent the observed behavior by using them to simulate behaving flies and to compare their simulated behavior to the behavior of observed, real flies. Simulated flies decide how long they want to stay in the current arm of a simulated Y-maze and whether they want to turn left or right, when leaving the current arm. The decisions are made by sampling the escape duration from a log-normal distribution with a time-dependent mean μ_t and stationary variance σ^2, and the left-right turns are sampled from a Bernoulli distribution with a time-dependent rate ρ_t (Methods). The mean μ_t of the escape duration distribution depends on the color of the arm and the presence of shock at the time point t. In addition, the mean escape duration can change with a reinforcement learning rule, which depends on the presence of shock. Also, the rate ρ_t of turning left or right can change with a reinforcement learning rule. The model parameters can be grouped into "static preference" parameters and "learning rate" parameters (Methods; Table S6). To assess the effects of genetics, learning and individual life experience, the parameters are fitted to the data in four different ways. First, all flies of the same genotype have identical parameters, but different genotypes have different parameters (*no individuality* model), thereby omitting the effect of prior experience or variability obtained prior to expressing a behavior (for example through developmental stochasticity). Second, parameter i of an individual simulated fly is sampled from a normal distribution with genotype-dependent mean $m_i^{(g)}$ and standard deviation $s_i^{(g)}$ (*individuality* model); these simulated flies have individuality in the sense that their behavioral policies differ from one another, because no two flies have the exact same parameters. In other words, simulated flies start the task as if in addition to their genetics, their life experience prior to the task (including stochastic processes during development) had shaped their individual behavior. Third, parameters are sampled as in the *individuality* fit, but the learning rate parameters

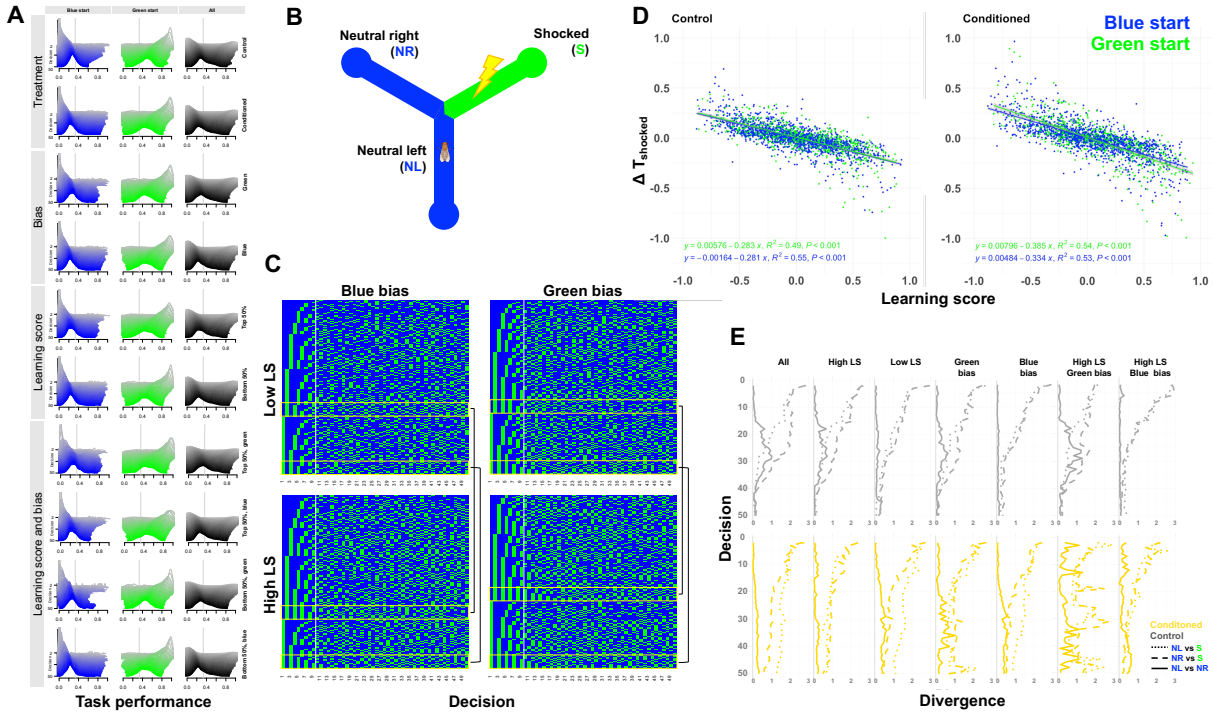

Figure 3. Divergence in individual task performance depends on learning through experience. A) Evolution of individual task performance distributions over the first 50 decisions is dependent on starting color. Task performance is shown for all flies, those who share the same color bias, and those with above and below average learning score. Lighter colors indicate distributions at earlier decisions. For blue starting color, two distributions are overlaid, one for flies starting at neutral left and the other for neutral right arm of the maze (see B). Only flies that made at least 50 decisions are included. Distributions of all flies regardless of starting position is shown in black. **B)** Schematic of the Y-maze and possible color and shock experiences. For the conditioned flies, the green colored arm (S) is associated with the shock, while the other two, blue arms are not (NL - neutral left and neutral right - NR). The green arm is also not associated with the shock in the control flies. **C)** Bias and learning shape the sequence of decisions. First 50 decisions in flies with high and low learning score and different color bias are aligned between individual flies (rows) and sequentially sorted. The yellow rectangles bring attention to flies with most persistent color choice switching behavior at the beginning of the task. Black brackets indicate flies that share the same first decision and hence can be compared across groups. The group of flies with unfavorable bias and with high learning score (bottom right) are more prone to initial switching color decisions for a prolonged time. **D)** Change in individual task performance from the start to the end of the experiment is more sensitive to experience at the first decision (blue or green color) due to learning. Note the change in slope of the association between learning score and the change in performance when the flies start the task at different colors in conditioned group (right panel). This effect is absent in the control (left panel). Each point is an individual fly. **E)** Evolution of residual individuality in task performance is sensitive to initial experience and exacerbated by opposing forces of learning and unfavorable bias. Evolving *shape Div* in H_{resid} is shown for task performance of flies starting at different arms of the Y-maze that made at least 50 decisions.

are set to zero, such that the presence of shock or color induce no lasting change on their behavior beyond the immediate effect of changing the escape duration (*no learning* model). Fourth, parameters are sampled per individual, but there is no genotype dependence of the means m_i and standard deviations s_i of the parameter distributions (*no genetics* model). In this case, the effect of genetics is omitted, including its effect on developmental variability.

Without individuality, i.e., with identical flies per genotype, the simulated flies fit the data much worse than with individuality (Figure 4A-B). Particularly striking was the mismatch in the distribution of the number of decisions the simulated flies had made within 20 minutes compared to the actually measured distributions of the number of decisions made by real flies (Figure S11). With individuality, but without genotype effects, the simulated flies were also clearly not recapitulating the observed behavior of real flies as well as when they were simulated assuming genotype-specific effects (Figure 4B). The difference between simulated flies with and without learning was smaller; in fact, for some genotypes, the model without learning had a lower Bayesian information criterion (BIC) than the model with learning (Figure 4A). However, we found that there were subtle changes in the observed data that the model without learning could not capture. In particular, we found that learning is an important factor shaping the change in task performance $T_{shocked}$, the overall decrease of the escape duration and the change in handedness from the first 5 minutes to the last 5 minutes of the experiment (Figure 4C). Further, the excess of non-Gaussian distributions of individual behaviors within a genotype in conditioned treatment could not be recreated in *no learning* model. This phenomenon was captured by the *individuality* model, even though this model draws parameters that characterize individuality strictly from normal distributions (Figure S5), reaffirming the effects of learning on residual individuality. Lastly, visual inspection as well as repeated simulations revealed that the distribution of simulated task performance matches the observed distribution better for the model with learning than the model without learning (Figure 4D, S11-12). These results confirm our conclusion that genetics and learning, make an essential contribution to expressed behavioral individuality as well as to the excess of residual individuality observed in conditioned genotypes. However, individuality is most dominantly sourced from non-genetic processes experienced before the behavior is measured. The fitted models allowed us to estimate how different the momentary task-relevant behavior of a given fly is compared to other flies, or how it compared to other moments in time (Methods). A visualization of these differences with multidimensional scaling revealed that the behavior of individual flies does not cluster according to genotype throughout the experiment, despite the fact that genotype-specific parameters were necessary to appropriately model the observed behavior (Figure 4E). The pairwise behavioral policy differences also suggested that the individual behavior had changed during the experiment, both in the control and conditioned treatment (Figure 4E-F). Further, we found that this change was slightly yet significantly bigger in the conditioned flies (Figure 4F, S13).

Given the observed changes and lack of clustering, we hypothesized that it would be difficult to infer the genotype purely based on the behavior of a single fly. Indeed, with a long-short term memory (LSTM) classifier applied to the behavioral data of individual flies, we obtained a low test accuracy of 3.4% (4-fold cross-validation). While this result was still above chance level (1.1%) and slightly above the 3% test accuracy that can be obtained with a feed-forward classifier applied to the number of decisions of individual flies (Methods), it also clearly illustrated that individual behavior is primarily a consequence of genotype-independent life events. In conclusion, our experimental data, models, and simulations demonstrated that the measured individuality of momentary behavior is genetically seeded, individually distributed across individuals, and then further substantially diversified within each genotype through a loop of individual learning from uniquely evolving life experiences which are themselves dependent on genetic and learned biases. Most importantly, we experimentally show that the preponderance of an individual's momentary behavior is not defined primarily by the genotype, present learning, nor the momentary circumstance. Rather, it is modeled from the accumulation of life-long, individual experiences that give rise to individual, and unpredictable behavior.

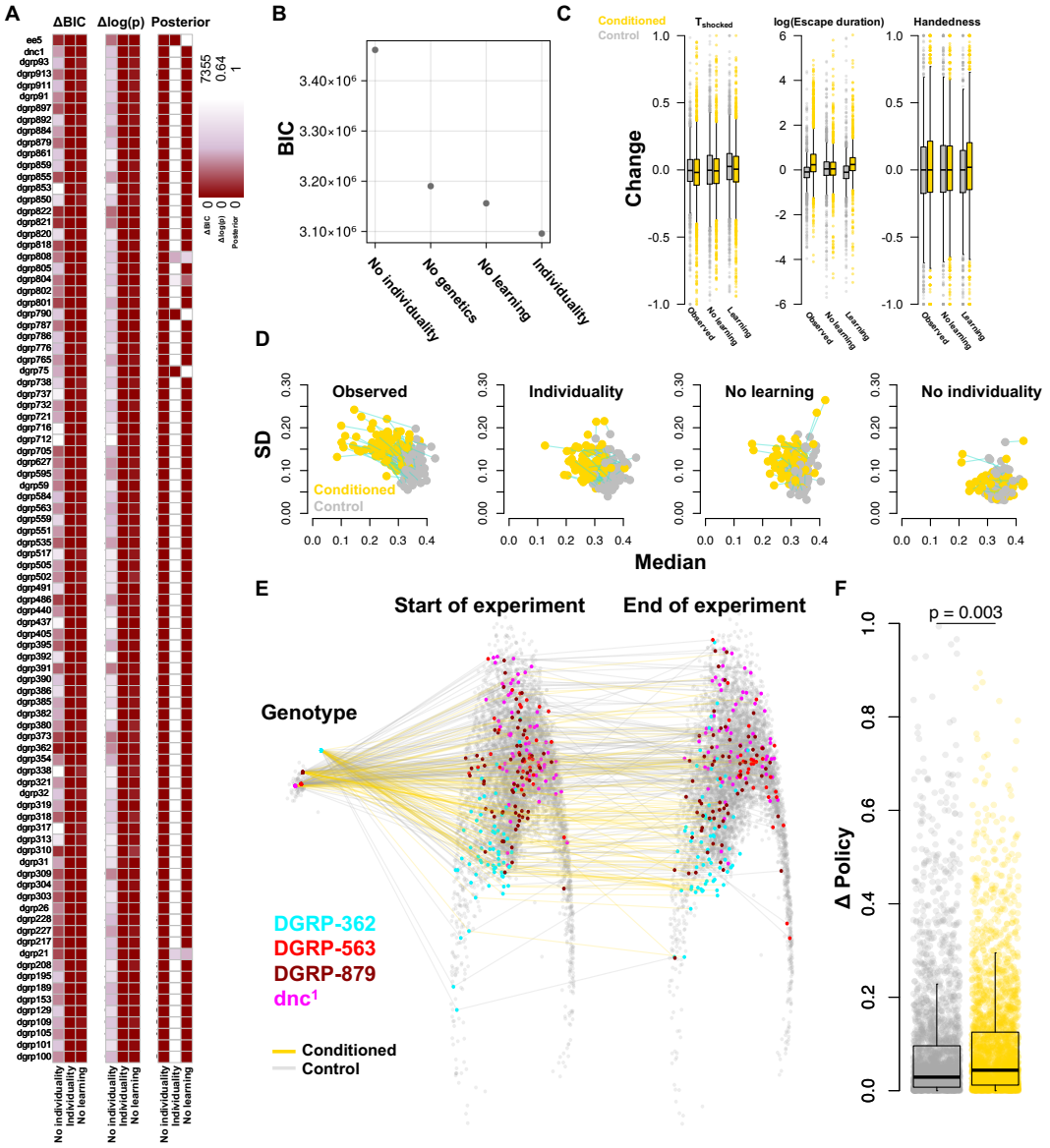

Figure 4. Experience, genetics and learning shape individuality. A) Variation in behavior observed across genotypes is best explained by a model that includes genetically controlled but individually random prior life experience, and learning. **B)** High Bayesian information criterion for models omitting the effects of prior individual variability, genetics and learning demonstrate that genetic effects on trait mean and variance and learning, as modeled in the *individuality* model, are necessary for close *in silico* recapitulation of observed behavioral diversity. Behavioral individuality is affected by variability in behavior obtained prior to the task, effects of genetic on the mean and variance of the behavioral expression and the effects of learning, in that order. **C)** Change in individual behaviors during conditioning can be attributed to the effect of learning. Boxplots summarize the behaviors of observed, real flies and of flies simulated with and without learning. **D)** Flies simulated under the assumption of genetic control over past life experience, and with learning can reproduce task performance behavior most consistently with the observed, real flies. (Other behaviors are shown in Figure S11.) **E)** Genetic effect on behavioral policy projects to the entire individual behavior space. Mean genotype policies and overlapping individual policies measured at the start and at the end of the experiment are projected on a multidimensional scaling plot and demonstrate almost complete unpredictability of individual behavior given the genotype in a controlled environment. Highlighted points correspond to individuals from an outlier genotype (turquoise), two average genotypes (red and dark red) and memory-deficient genotype (magenta). **F)** Significant change from initial behavioral policy occurs in conditioned flies during the 20 minutes between the start and the end of the task experiment. Each data point in D) represents a genotype × condition. Each point in E) and F) represents an individual.

Discussion

Behavioral genetics is grounded on the notion that behavior is fundamentally determined by genetics[1] and its deterministic interaction with the environment. In support of this, the discovery of numerous genes that affect behavior demonstrated that large genetic perturbations in a fixed environment can cause measurable, replicable and predictable perturbations in behavior[e.g. 19,20]. While we show both experimentally, through data-driven heuristic modelling and through simulations that the genetic background indeed plays an essential role in shaping the behavioral individuality in a cognitively challenging task, our summarized results are clearly at odds with the presumed relative importance or predictive power of genetics. This is because we found that genetic control over learning-dependent behavior contributes only to the extent of possible expressions of individual behavior. Genotype only provides a range of individual behavioral seeds which determine unique, learning-independent, individual experiences. Importantly, unlike in the case of severe artificial genetic perturbations, the genetic impact on the extent of individuality largely overlaps between natural, genetically highly diverse populations. This result is one of the rare experimental confirmations of what has been hypothesized or assumed about the individual learning-dependent behavior: despite that we know the behavior is under some deterministic, genetic control, the individual, experience-based behavior is in fact not predictably defined by genetics. We see this most vividly in the overlapping ranges of individual task performances and behavioral policies of 90 genetically highly diverse, wild-type and laboratory genotypes. All of these genotypes could produce almost any individual behavioral phenotype within a shared, experimentally controlled environment. And yet, we also find these ranges cannot be reproduced without assuming diversity in genetic control. This, perhaps inconvenient truth has already been intuited by many experimentalists measuring learning-dependent behaviors - even in presumably perfect experimental conditions, behavioral variability is imminent. This has severe implications for how we approach the study and interpretation of cognitive behavior. Even under experimental control over the environment, genetically identical individuals will be cognitively unique and behaviorally unpredictable. Their individuality can be exacerbated even by minimal variation in individual experience. We found such minor events, often created by the behaving agent itself, can modify future behavior and snowball the divergence of individuality. To understand the mechanistic intricacies of cognition, we therefore cannot rely on averaged, linear measures of behavior within a species, or at least not within one generation. Cognitive behavior has to be assessed on an individual, whole-life basis because it is temporally dynamic and non-ergodic due to experience, learning and memory. This is especially true in natural settings, where environmental complexity experienced over time immeasurably exceeds the complexity experienced over 20 minutes in a simple two-color Y-maze. The combinatorics of sequential, time-dependent experiences across genetically diverse individuals in nature will tend to infinity, and, extrapolating from the results of this study, the true predictive power of genotype on individual behavior will tend to zero. Practically, this means that in non-experimental setting, the concept of genetic determinism of cognitive behavior is predictively futile. Our study provides experimental evidence for a scientifically as well as ethically and societally important conclusion that individual behaviors cannot be evaluated based on genotype or momentary circumstance, but based on whole-life experience. Thanks to the advancements of high-throughput, high-resolution phenotyping and genotyping technologies, the scientific community should continue pushing onward with the systematic exploration of the fundamental processes and mechanism that shape individual cognitive behavior, including genetics. This may lead us to discover basic concepts underlying the architecture, emergence, and pathology of individual cognitive behaviors, and, perhaps some day, its improved predictability, albeit only within increasingly sophisticated and controlled experiments. Extrapolating and translating from this knowledge will enable us to design better, biologically inspired artificial intelligence systems and improve our understanding of natural yet experimentally inaccessible cognitive systems. However, we need to become aware of the fact that genetics cannot be used to assess present or future behavior of an individual, especially in cognitively complex, long-lived animals behaving in diverse environments and societies, such as humans.

Methods

Y-mazes

Behavioral arenas were 3D printed in black Tough PLA (Ultimaker B. V., Utrecht, Netherlands) using desktop Fused Deposition Modeling (FDM) 3D printer (Ultimaker S5, Ultimaker BV, Utrecht, Netherlands), with a z-axis resolution of 0.1 mm, and 100% grid infill pattern. The mazes are in the form of the letter 'Y', with equal arm lengths. The arms are connected at the center with an angle of 120° from each other, and length = 10 mm and width = 2 mm. This specific arm width was chosen so that the flies are not able to turn around in the middle of the arm. This way the fly must traverse the whole arm and reach the end, where it is provided with a circular turning area of a diameter = 4 mm. This is done so that the fly, after making a decision, remains in the arm for long enough to associate the electric shock with the color of the arm. For the same reason, the fly only gets shocked once it has entered an arm with its full body length, and not at the junction of the three arms. The same requirement is implemented for the removal of electric shock - the fly needs to exit the shocked arm but also enter the non-shocked arm with the full body length in order to escape the shock (Figure 2). The total height of the maze within which the fly is restricted is 1.2 mm. The wall

of the maze does not erect straight up to the ceiling, but in a cross-section forms a step at 0.8 mm. This is done so that the fly, once resting on the floor of the maze, is not able to climb up to the ceiling of the maze and avoid getting shocked. The ceiling of the maze is a regular 25 x 75 mm glass slide coated on one side (facing the maze) with dry Polytetrafluoroethylene (PTFE) aerosol (KONTAFLON 85, Kontakt Chemie, CRC Industries Europe BV, Zele, Belgium). The coating makes them hydrophobic, and hence, slippery for the flies to walk on. Each slide covers two Y-mazes horizontally. Eight Y-mazes (4 rows x 2 columns) are 3D printed together, with each Y-Maze restricted within an area of 30 mm x 30 mm, which corresponds to an individual shocking area on the transparent shocking grid (described in the next section). A single plate consisting of 8 Y-mazes is then laid over, and glued onto a transparent shocking grid. Eight such arenas (64 Y-mazes) are placed on top of the LCD for the assay.

Conditioning platform

Indium tin oxide (ITO) coated (400 nm coating corresponding to 4-6 Ω/sq) glass plates (150 mm x 100 mm x 1 mm), were laser etched to form a grid of 8 (4 rows x 2 columns) isolated 30 mm x 30 mm shock delivery pads for each Y-maze. The shocking pads were patterned in the form of an interdigitated grid, with a central pad connected to the ground, and 8 isolated pads connected to an array of normally off electromagnetic relays. Each isolated pad was etched in an interdigital pattern with 15 digits of 1 mm width on each side (ground pad, and active pad connected to the relay) separated by a distance of 20μm between each digit. Holes (diameter 0.8 mm) were laser cut into the glass plate at positions that correspond to the center point of the circular ends of the Y maze arms. The holes are used to deliver CO_2 to anesthetize flies for fly retrieval at the end of the assay. The designed plates were manufactured at Diamond Coatings Ltd., UK. The 3D printed Y-mazes are assembled with the glass plate using adhesive tape or superglue, making sure the glue does not touch the ITO coating. Each such assembled plate is placed on a 3D-printed holder fixed on top of an LCD screen (LG 25BL56WY, 25", 1920 x 1200 pixels). The holder can hold 8 glass plates and is fitted with grooves for electrical wiring and place marks for copper tapes (12 mm width) (Figure). Copper tape is applied on the glass plates to make electrical contact between the ITO pads and the copper tapes on the holder. Custom-made printed circuit boards fitted with 5.1 mm round head gold spring contacts (P/N 5099-D-2.0N-AU-1.3C, PTR Hartmann, Germany) electrically connect the copper tapes to the electromagnetic relays, ultimately connecting it to each isolated shocking area. Electrification of the 8 isolated Y-mazes is controlled by an array of 8 relays, which in turn is controlled by an 8-bit shift register (TI 74HC595). The 64 mazes are controlled by 64 individual relays, which are controlled by 8 shift registers. The registers are controlled by the computer program (testY_LCD.py) via an Arduino Mega 2560 Rev. 3 (ATmega2560) (loaded with Arduino_yMaze_shock_595.ino) in closed loop with the position of the fly inside the maze and the visual stimulus presented to it via the LCD screen. Visual stimuli can be, but are not limited to, colors, color gradients, patterns or light intensities. The whole system is made to be modular, and the plates holding the Y-maze arenas wireless, so that it is not fixed to the LCD screen. This way it can be moved around for the purpose of fast loading the arenas with flies. When electrified, the floor of each maze delivers a constant 30 V DC through the flies legs. The current is limited to 500 mA distributed between 64 arenas (on average 7.8 mA per fly) and powered using a benchtop power supply (RND 320-KA330-5P, RND Lab, Switzerland). The electronics circuits are powered using a 5 V, 90 W switch mode power supply (LRS-100-5, Mean Well Enterprises Co. Ltd., New Taipei City, Taiwan). This current was chosen through optimization experiments in which the goal was to maintain reproducible shock avoidance in flies across several randomly chosen wild-type genotypes, while the memory mutant *dnc*^{1} flies, that usually experience most shocks due to their inability to learn, do not get injured during the experiment.

Closed-loop control

Each Y-maze is associated with an Augmented Reality University of Cordoba (ArUco) marker[64], which is identified by the control software (getBoxes_aruco_64.py) to acquire the position of each maze. This is done both to automate the experiment and to maintain the accuracy in case of an accidental misalignment of the plate within the tolerance of the plate holders when setting up the experiments. The position of each moving fly is captured using a custom background subtraction algorithm (unit_fly.py), and fed into the control algorithm (testY_LCD.py, unitMaze.py). In turn the algorithm changes the visual stimulus presented to each fly via colored patterns on the LCD screen (LCD.py). The algorithm also controls the electric shock delivery for each fly via an Arduino Mega 2560 Rev. 3 in real time (Arduino_yMaze_shock_595.ino). The platform is illuminated with an array of 12 x 8 infrared (940 nm) LED (Figure 1). The video is captured at 6 fps using a grayscale industrial USB 3.0 camera without an infrared filter (DMK 38UX253, The Imaging Source, Germany), fitted with an infrared long pass filter (dia. 40.5mm thread, 0.5 mm, 093 IR Black 830, Schneider Kreuznach GMBH, Germany). The filter allows the program to ignore any background illumination changes inside the room that can interfere with the accuracy of the fly detection algorithm. The program is generally robust to light interference caused by movement around the setup, but to minimize any potential light interference, as well as to minimize influencing flies' behavior the experimenter left the room during the assay or wore black or dark clothes. Different associative learning protocols can be implemented with this system, whose codes can be found on our GitHub repository https://github.com/jaksiclab/GeneticsOfLearningIndividuality. At the end of each protocol, the program outputs a folder containing comma-separated values (.csv) files reporting the data acquisition times (in nanoseconds starting

from the time of acquisition of the first fly position), the coordinates of the fly, the arm in which the fly resides at each moment, whether the arena is electrified or not, the correct, incorrect and total number of choices the fly has made at that point of time. The program also automatically outputs the final task performance scores of the flies at the end of the experiment, the time at which the experiment was performed, sped up infrared video recordings of the arena (.mp4) and setup metadata that needs to be input by the user at the start of the experiment. For further automation, this information can directly be accessed by the control software immediately after an experiment.

Drosophila stocks and rearing

All genotypes were acquired from the Bloomington Drosophila Stock Centre (BDSC) in the year 2020. 88 Drosophila Genetic Reference Panel (DGRP) lines, norpA^{EE5} (BDSC stock number 5685) mutants, and *dnc*^{1} (BDSC stock number 6020) mutants were used in this study. DGRP genotypes are denoted by a number (*nnn*) or a label *DGRP-nnn*, where *nnn* represents the DGRP genotype. For example, in Figure 2C and 2G, genotype was denoted as for 208 or DGRP-208, respectively, and both indicate that the genotype used was DGRP-208 line (synonym RAL-208; BDSC stock number 25174). Flies were maintained and raised on cornmeal agar medium: 6.2 g agar-agar, 58.8 g cornmeal, 58.8 g brewer's yeast, 0.1 L grape juice - Migros M-Classic, 4.9 mL propionic acid, 26.5 mL methylparaben Moldex, 1 L of tap water (Lausanne, Switzerland). Environmental temperature was 26°C (± 0.5°C), humidity 50% RH (±5%), and circadian light condition was set to 12 hours light/dark cycles (instant switch, no ramping). The maternal generation (F1) was generated in three vial replicates from eggs laid by two sets of F0 flies taken from stock vials. F0 stock vials that were maintained at 21 °C (± 1°C), on the same medium, but with no circadian light control. Stock populations varied between 20 and 60 flies per vial with no larval density control. Nine F0 females and 5 F0 males were selected from stock population, housed together and allowed to lay eggs for 3 days, after which they were discarded. The vials were checked periodically to ensure the development was healthy and progressing at an expected pace. While we set up 3 replicate vials initially, only two were used - the extra vial served as back-up for the cases when a vial needed to be discarded. Any vial showing signs of distress, such as dry food, biofilm, too few larvae or pupae or crowded vials were discarded and the rearing protocol was restarted from the beginning, unless a backup vial was available. This was assessed always by the same experimenter. The F1 progeny were collected 12 days after the last day of egglay. The experimental F2 generation was set up from each vial replicate the same way as the F1 generation. However, after discarding the F1 adult flies, and after 9 days of development, the vials were checked for eclosion daily. As the first few flies eclosed they were discarded. The next day, the peak eclosion would follow, and the newly eclosed flies were collected. Around 40 males and 40 females were then separated into two vials with fresh medium and prepared for the behavior assay that would follow 3 days later, when the adult flies were 5 days old. All the preparatory flywork, including collection, sorting and counting flies across the generations was performed swiftly and using light CO_2 anaesthesia (5L/min flow through standard CO_2 pad) at laboratory room temperature, 21°C (± 0.5°C). All flies were handled by a single experimenter (by R.M. for the single day experiments, and by G.V.B. for multi-day experiments).

Operant conditioning

We use two operant conditioning paradigms, the associative visual place learning (Figure 1C), and the associative color learning (Figure S1A). In both paradigms, the unrestrained fly can explore the Y-maze and make sequential binary decisions at the junction of the three arms. Conditioning is initiated after initial measurement of unconditioned behavior. The decisions during conditioning can result in the absence, introduction or removal of foot shock (Figure 1A, S1A).

For each genotype, we used two biological replicates, progeny of two different sets of males and females, that were reared independently in different vials. Each replicate consisted of 32 flies, equally split between males and females and between two treatment groups, conditioned and control. Environment during conditioning was kept the same as for rearing. Flies were very lightly anaesthetised (10 L/min CO_2 flow on 30 x 40 cm custom-made CO_2 pad) and loaded into the Y-maze arenas using an aspirator. In the conditioned group, flies underwent operant conditioning in the presence of shock, while in the control group the flies were allowed to spontaneously explore the maze experiencing the same visual and environmental stimuli, but without experiencing any shock. All flies were tested during the same "non-siesta" circadian timeframe (20% ZT 0-1, 30% ZT 1-2, 30% ZT 2-3, 15% ZT 3-4) with exception of around 4% of flies extended beyond ZT 3 (3% ZT 4-5, 1% ZT 5-6 , 1% ZT 6-7) due to technical issues; Table S1). We found no difference in task performance given the zeitgeber timeframes (ANOVA (Task performance Ẽxperiment time (ZT) * Treatment) p = 0.531).

During this time, flies tend to make on average 76 decisions per 20 minutes, with more decisions made by males (N_{male} = 82, N_{female} = 62), and fewer decisions made in the presence of conditioning ($N_{control}$ = 89, $N_{conditioned}$ = 63). In the place learning assay, one of the three arms of the Y-maze is colored differently from the other two, and an electric shock is associated with that color. The colors chosen are blue and green, as flies have been shown to be able to distinguish well between the two in previous associative learning studies[65,66]. At the junction of the Y-maze, the fly is presented with a binary choice between two arms. When conditioning to avoid the color green, the fly gets shocked when it enters a green arm, while the shock is stopped

when it leaves the green arm and enters a blue arm. No conditioning occurs when it enters a blue arm from another blue arm. Hence, we are implementing a combination of positive punishment (adding aversive stimulus following incorrect behavior), and negative reinforcement (removing aversive stimulus following correct behavior). The shocked arm was associated with a color assigned to different arms in a clock-wise way, column-wise across the 64 mazes (Figure 1B), and kept fixed for the entire place learning assay. In the color learning assays the shock arm was associated with a color, but the color of the arms changed with every decision, making the shock and the color uncoupled from a position in space. At the start of any assay, the entire arena is illuminated with red color for 2 seconds while the floor becomes electrified. This moves the flies from a state of rest to a state of arousal. The video recording is initiated and for the next 3 minutes, the fly is allowed to explore the maze and get accustomed to it without delivering any shock. This time is also used to assess prior individual biases and initial fly behaviors. The operant conditioning assay is then initialized and recorded for 20 minutes.

Experimental validation of the Y-maze conditioning assay In the place learning paradigm, wild type conditioned flies spent an average of only 10.5% of the total assay time in the shocked arm, while the control group spent significantly more time in this arm in the absence of shock ($T_{shocked}$ = 32.5 %, Student's T-test p = $2.52e^{-10}$). The learning-deficient (*dnc*^{1}) showed poor relative task performance at avoiding the shocked arm (conditioned $T_{shocked}$ = 27.8 %, control $T_{shocked}$ = 30.8 %; p = 0.20). Similarly, relative task performance of visually impaired (*norpA*^{EE5}) was low (conditioned $T_{shocked}$ = 25.4 %, control $T_{shocked}$ = 25.0 %; p = 0.90; Figure 1), suggesting that in flies visual context such as color is informative for place learning[67]. Alternatively, the *norpA*^{EE5} mutation may also induce learning impairment beyond perceptual deficiency[68].
While average genotype performance was consistent across learning paradigms (Figure S1, S2), across different color stimuli (Figure S1, S2), and, across consecutive measurements of same populations over multiple days (Figure S2), we find that individual learning task performance is variable and evolves over time (Figure 2, S2, S3).

Multi-day learning task

In the multi-day learning task, genotypes DGRP-362 and *dnc*^{1} were reared based on the standard rearing explained above but in 12 replicate vials per genotype (3 replicate vials per experiment type, except for *dnc*^{1} for which we had two instead of three replicates for the last two experiments, because two vials were discarded due to poor development). 256 individuals from the two genotypes were collected (total N = 512 flies) to be tested in four types of experiments. Before the test, the collected flies were housed in fly vials in groups of around 40 individuals of mixed sexes. On the day of each first test, 32 females and 32 males were selected for the test. In each of the four experiments, a set of 64 individual flies were tested once per day with the exception of the second experiment of DGRP-362 that contained 59 flies (32 males and 27 females) due to experimenter error (fly identities were accidentally and intractably swapped). In total N = 507 flies were tested successfully. Flies were tested on two consecutive days followed by one day without a test, then another set of two test days. All tests were done under conditioned treatment. Before each conditioning session, flies were allowed to explore the arena for 5 minutes in the absence of shock. A 20-minute conditioning session ensued, followed by a 5-minute session in the absence of shock, to assess change in bias due to learning and short-term memory. This regime was repeated once per day, at the same time of the day (Zeitgeber 0-2). In the first experiment (PPCC_gbgb), flies were tested in a place learning paradigm the first two days ("PP"), then in the color learning paradigm the last two days ("CC"). The colors associated with the shock across four days alternated across tests between green and blue ("gbgb"). In the second experiment (PPCC_bgbg), they alternated between blue and green. In the third (CCPP_gbgb) and fourth experiment (CCPP_bgbg), on the first two days place learning was tested, and on the last two days, we tested the flies in a color learning paradigm. The colors associated with the shock alternated the same way for the third and fourth experiment, as in the first and second, respectively. Between tests, identity of each fly was tracked by housing them individually in a custom 3D-printed 64-well single housing plate, placed on food and isolated with a dome to avoid the food from drying up. The flies were transferred to the single housing upon completion of the each test. Each fly was always tested in the same Y-maze on the platform over the days. The position in the well plate corresponded to the position on the platform to facilitate quick set up of the experiment. Males were placed on the top 4 rows of the platform and females on the 4 bottom ones. All flies were handled by a single experimenter (by G.V.B.), except for the third experiment (where the assay was set up by A.M.J.).

Single fly housing

The single housing plate used in the multi-day learning task consists of 64 cube-shaped wells, organized in 8 rows and columns. The floor of the plate is a 0.2 mm thick printed mesh. The mesh allows the flies to reach food and eat when the plate is placed on a tray filled with fly medium, while keeping them as dry and clean as possible throughout the experiment. Care should be taken to only gently press the well-plate on the surface of the medium and prevent food from entering the wells. The mesh also helps with anaesthetising the flies by simply placing the plate onto the CO2 pad. The top of the 64-well plate is covered with a 3D-printed lid, shaped as an inverse imprint of the 64-well plate. This way, when it covers the well plate, the grid of the lid protrudes by 0.2 mm into each well, preventing the flies from wiggling their way between the

lid and the plate and crossing into another well. A thin, fine filter mesh, usually used for Drosophila egg collection, was printed into the top printed layers of the lid. To manufacture this, the top four 0.06 mm layers of the lid are printed first. Then, the printer is paused, the filter mesh is laid over the printed part and tightly affixed to the printer's build plate with an adhesive tape. The printing is resumed so that the next layers of print material "bakes" the mesh into the print. After printing, the mesh remaining on the outer part of the print is cut with a precision knife. The .stl models can be found in the github repository. The plate and lid were printed using red PLA filament (to avoid color imprinting or color bias) on an Ultimaker S5 3D-printer. Black filament can be used as well, but the low contrast with the fly makes picking and placing flies from the well more challenging and prone to errors. The 3D models were sliced with Ultimaker Cura, using default "Fine resolution" print setting (0.06 mm layer height). To create the bottom printed mesh, we use Ultimaker Cura slicer to slice a 0.2 mm thick block with width and length matching the size of the dimensions of the 64-well plate. We use the 60% "grid" infill and omit the bottom and the top layer print. Once printed, the mesh is glued to the bottom of the 64-well plate using cyanoacrylate adhesive. This has to be prepared at least 24 hours before the experiment, in a well-ventilated room, to allow the volatile compounds of the adhesive to fully air out. Occasional slight warping of the lid would make it possible for flies to cross to other wells, thus losing track of their identity. Thus, testing the lids before an experiment is advised.

Basic statistics

All basic statistical tests were performed within the R environment (R version 4.0.2.). Pearson correlations and T-tests were performed using base cor.test() and t.test() functions. T-tests were two-sided. Resampling test was performed using the function lmperm() from the package permuco[69]. Exact general independence test was performed using the function independence_test() from the package coin[70,71]. Generalized linear mixed models were fitted using lmer() function from the lmerTest package and the analysis of variance for fitted models was performed using the anova() function. Least square means and the pairwise difference between them were calculated using emmeans (pbkrtest.limit=100000000) and pairs() function from lsmeans R package. Where multiple tests were compared p-values were corrected using Bonferroni correction for multiple test using base p.adjust(method="bonferroni") function. Density distributions are estimated as kernel densities using density() function and default parameters.

Definitions of behaviors and other behavior-based measures

Task performance ($T_{shocked}$) of a fly is the fraction of time a fly has spent in the conditioned arm during the length of the experiment (20 minutes). It is measured the same way regardless whether the shock is applied or not (for example in the control experiment). *Handedness* of a fly is the absolute value of the total number of right turns subtracted from the total number of left turns, divided by the total number of turns taken by the fly at any given time frame. *Developmental noise* is the absolute handedness of a fly measured during the three minutes prior to the conditioning. *Velocity* in mm/s for a given time frame, is calculated by averaging the displacement of a fly per second over the said time frame. *Relative velocity* is the difference in average velocity of a fly between the shock-associated arm of the Y-maze and the neutral arm of the Y-maze at a given time frame. *Shock response* is the absolute value of the difference between the average velocity of a fly measured during the three minutes prior to the start of the conditioning part of the experiment and the average velocity of the fly during the first quarter (5 min) of the conditioning experiment (when shock becomes implemented in the conditioned group). *Color bias* of a fly is defined as the total fraction of the time the fly spends on the color during a set time frame. *Percent correct decisions* is the proportion of made decisions to enter the non-shocked arm out of all made decisions to enter any arm. *Learning score* is computed by splitting the experiments into 10 bins of 2 minutes and computing the negative of the average of two Spearman's rank correlations: 1) the rank correlation of the interval index *i* with the relative time spent in the shock arm during interval *i* and, 2) the rank correlation of the interval index *i* with the relative number of visits to the shock arm during interval *i*.

Genotype-specific relative task performance

Before calculating mean task performance for a genotype, we first filter out individual flies based on their lack of activity. Flies are removed from the analysis if they remain at the shocked arm for 3/4 of the experiment or if they never enter the shocked arm/color (in either conditioned and control group of flies). Based on observations in trial and final experiments, this outlier behavior was due to the fly getting accidentally injured by mis-manipulation during assay setup (usually by slightly misplacing them outside the maze boundary and pinching them with the glass slide). The filtering accounted for 3.78 % of all tested wild-type flies. A linear mixed modelling is then used to estimate the effect of genotype on the response to shock and to regress out nuisance factors that may affect the measures of learning. Those included sex, replicate, sex-specific locomotor activity during and in the absence of shock, developmental noise, position of the Y-maze, position of the shocked arm, position of the arm in which the fly initializes the task. The model with the $T_{shocked}$ as the response variable, genotype interacting with the treatment (conditioned or control), sex, developmental noise (absolute bias locomotor handedness), shock response and the starting arm (shock or neutral left, or neutral right) as the fixed effects, and the replicate number, and the position of the fly on

the 64-maze arena as the random effects, is fitted to the data to capture individual components of variance of the data (Table S2, S3). The least squared means of the genotype x treatment effect was extracted. Relative task performance of a genotype was measured as the Tukey's Honestly Significant Difference in least square mean of $T_{shocked}$ for a genotype in the conditioned group and least square mean of $T_{shocked}$ for a genotype in the control group.

Individuality Extent of expressed individuality in a behavior within a group of flies is measured using the differential entropy[72] of the probability distribution function of the behavior for that particular group, estimated over the theoretical range of the behavior (Table S5). For Gaussian distributions, entropy scales with the logarithm of the standard deviation and is thus consistent with classical measures of variability in isogenic populations, often called individuality (Figure S14). The difference in expressed individuality between two groups of flies is calculated as Hellinger distance[73] between the two distribution functions. Specifically, we calculate Hellinger distance between two continuous probability density functions of the distributions, over the theoretical range (Table S5) of the concerned behavior.

Residual individuality and shape divergence

To assess the extent of residual individuality (H_{resid}), the distributions of expressed individual behaviors within genotypes, groups, or replicates are first independently divided into a histogram of 10 bins within the individual range specific to each distribution. The probabilities of finding a measurement in each of the 10 bins are then calculated to obtain the binned probability distribution, based on which the Shannon entropy[74,75] is calculated. The H_{resid} correlates negatively with the range of $T_{shocked}$ (Figure S14). This is a result of scaling the distributions within their own ranges, and is consistent with our definition of H_{resid} being free from the effects of environmental and developmental stochasticity. That is, assuming we are able to capture the full range of the expressed behavior (evidenced by consistency of the distributions between replicates), a group of flies having a narrow range of $T_{shocked}$, will be scaled to an approximately uniform distribution within the range of the particular distribution (Figure S7), and hence, have a higher entropy. To capture the difference in expressed residual individuality between two groups, the same independent binning approach is taken for each group-specific probability distribution separately, and the Kullback-Leibler (KL) Divergence[76,77] of the two distributions is calculated. Since each distribution is binned independently within their own range, every distribution becomes a list of 10 probability values (summing up to 1), with each value having an equal weight for the calculation of the entropy as well as the divergence. This procedure scales each probability distribution to a common range (Figure S7), and ensures that the entropy and the divergence measures are only capturing the shapes without being confounded by the central tendencies or the ranges of the distributions. Effectively, we capture residual individuality that is expressed independently of the variability caused by developmental stochasticity or environmental plasticity. The KL divergence is a non-metric, asymmetric measure of how different one distribution is from a reference distribution. Therefore, when we measure the change in the residual individuality as a result of conditioning (Environmental Variability *EV*), we measure the KL divergence of the conditioned (shocked) population with respect to the control (non-shocked) population. In other cases where no reference distribution is obvious, KL is calculated in both directions (comparison between genotypes within a treatment, Genotype Variability *GV*), or the compared distribution pairs are randomized, and the pairs are kept consistent between tested environments (comparison between replicates within a genotype and treatment, Measurement Variability, *MV*).

To provide an alternative measure of differences in the shapes of distributions that are symmetric or less sensitive to outlier values we also calculated Hellinger distance[73] and Jensen-Shannon divergence[?] between the distributions of $T_{shocked}$ in control and conditioned treatment, that were centered around the median. We also applied the KL divergence on non-binned, continuous distributions of $T_{shocked}$ (Figure S14). We found that these measures all correlate strongly and significantly with each other and with either the range, variance and entropy of the $T_{shocked}$ distributions and/or the relative task performance. While they do uncover various differences between distributions, these measures are not free from variance and central tendency effects. Hence, we refrain from using them for measuring the changes in *Residual individuality* (Figure S14).

Modeling behavior

To model individual fly behavior, we extract for each fly a sequence of arm identities $x_i \in \{1,2,3\}$, arm color $c_i \in \{\text{green}, \text{blue}\}$, presence of shock $s_i \in \{\text{shocked}, \text{not shocked}\}$, arm escape-duration $\Delta t_i \in \mathbb{R}^+$ and turn events $y_i \in \{\text{right}, \text{left}\}$. For example, the sequence $S = ((x_1 = 3, c_1 = \text{green}, s_1 = \text{shocked}, \Delta t_1 = 1.0\text{ s}, y_i = \text{right}), (x_2 = 1, c_2 = \text{blue}, s_2 = \text{not shocked}, \Delta t_2 = 3.5\text{ s}, y_2 = \text{left}), \ldots)$ means that a fly started in arm 3, perceived color green and got shocked, escaped arm 3 after one second by taking a right turn at the center of the maze, arrived in arm 1 with color blue and without shock, stayed there for 3.5 seconds and left it with a left turn, etc. We model the probability of a given sequence S of length T as $P(S) = P(\Delta t_T|\mu_T, \sigma)\prod_{i=1}^{T-1} P(y_i|\rho_i)P(\Delta t_i|\mu_i, \sigma)$, where $P(y_i|\rho_i))$ is a Bernoulli distribution with probability of turning right given by ρ_i and $P(\Delta t_i|\mu_i, \sigma)$ is a log-normal distribution with mean μ_i and standard deviation σ. The probability of turning right $\rho_i = \sigma(w_{x_i}^{(i)}) = 1/(1+\exp(-w_{x_i}^{(i)}))$, depends on the weights $w_1^{(i)}, w_2^{(i)}, w_3^{(i)}$ (one for each state). These weights change according to the following dynamics: $w_{x_i}^{(i+1)} = w_{x_i}^{(i)} + \left(\eta_g I(c_{i+1} = \text{green}) + \eta_s/(1+\phi_w n_i) I(s_{i+1} = \text{shocked})\right) \cdot (I(y_i = \text{right}) - \rho_i)$, where η_g is the green color learn-

ing rate, I denotes the indicator function with $I(\text{true}) = 1$ and $I(\text{false}) = 0$, η_s is the shock learning rate, n_i is a shock counter (number of times shock was experienced so far), and ϕ_w is a parameter that scales the dependence on the shock counter. This learning rule increases the probability of turning right in state x_i, when turning right led to the green arm without shock and $\eta_g > 0$ (color preference learning), and it leads to a decrease in the probability of turning right, when the negative impact of arriving in a shocked arm outweighs the preference for arriving in a green arm ($\eta_g + \eta_s/(1+\phi n_i) < 0$), and vice versa for turning left. The means of the log-normal distribution are given by $\mu_i = \mu^{(i)} + \Delta_g I(c_i = \text{green}) + \Delta_s I(s_i = \text{shocked})$, where the parameters Δ_g and Δ_s control the change in escape duration due to being in a green arm or being shocked, relative to the mean $\mu^{(i)}$. This mean changes according to the dynamics $\mu^{(i+1)} = \mu^{(i)} + \eta_\mu/(1+\phi_\mu n_s) I(s_i = \text{shocked}) + \eta_t \Delta t_i$. With this update rule, the mean of the log-normal distribution over escape durations can change simply with the passage of time, when $\eta_t \neq 0$, but also due to being shocked, when $\eta_\mu \neq 0$. To model a population of flies, e.g., 64 flies of the same genotype, we place normal priors over the model parameters (Table S6) and estimate the means and standard deviations of these priors with approximate expectation-maximization[78]. We considered four different models:

no individuality: all flies with the same genotype have exactly the same parameters, i.e., the standard deviation of all priors is zero ($k = 11$ parameters per genotype; (Table S6).

individuality: normal priors with fitted mean and standard deviation over all parameters, except the learning rates η_s, η_g, η_μ and the factors ϕ_w, ϕ_μ, which are shared across individual flies of the same genotype, as in the no individuality model ($k = 11 + 6 = 17$ parameters per genotype). Sharing the learning rates led to a lower BIC than a model with individuality in all parameters (not shown).

no learning: same as individuality, except that $\eta_s = \eta_g = \eta_\mu = \eta_t = 0$ and $\phi_w = \phi_\mu = 1$ ($k = 11 + 5 - 6 = 10$ parameters per genotype).

no genetics: all flies are fitted with the individuality model ($k = 17$ parameters), shared parameters due to genotype is not modeled.

Bayesian information criterion BIC and marginal log probabilities were estimated with 10^4 samples[78].

The difference in momentary behavior between two simulated flies was computed with the Hellinger distance[73] between the policies, averaged over all possible states.

Simulating behavior

We simulated tracks for 64 flies per genotype split equally between treatments based on the genotype-specific or individually fitted parameters from the different models.

Predicting genotype from behavior

To decode the genotype from behavior, we trained a recurrent neural network with one hidden layer of 32 LSTM cells with relu-activation on the behavioral sequences encoded as $(\text{onehot}(x_i), s_i, \Delta t_i)$. The feed-forward baseline model contained 2 hidden layers of 32 relu neurons with the input being the number of decisions encoded as 20 dimensional vectors with Gaussian tuning, i.e., for number of decisions n, input neuron i's activity is given by $a_i = \exp(-(n-c_i)^2/(2\cdot 10^2))$ with $c_i = (i-1)\cdot 20 + 2$.

Data availability

Data and code used to produce the main results, as well as PCB and 3D print designs will be made available on a github repository https://github.com/jaksiclab/GeneticsOfLearningIndividuality and on Zenodo upon peer-reviewed publication.

References

1. Harden, K. P. Genetic determinism, essentialism and reductionism: semantic clarity for contested science. *Nat. Rev. Genet.* **24**, 197–204, DOI: 10.1038/s41576-022-00537-x (2023).
2. Plomin, R. & von Stumm, S. The new genetics of intelligence. *Nat. Rev. Genet.* **19**, 148–159, DOI: 10.1038/nrg.2017.104 (2018).
3. von Stumm, S. & Plomin, R. Using DNA to predict intelligence. *Intelligence* **86**, 101530, DOI: 10.1016/j.intell.2021.101530 (2021).
4. Linneweber, G. A. *et al.* A neurodevelopmental origin of behavioral individuality in the Drosophila visual system. *Science* **367**, 1112–1119, DOI: 10.1126/science.aaw7182 (2020). Publisher: American Association for the Advancement of Science.
5. Taylor, L., Watkins, S. L., Marshall, H., Dascombe, B. J. & Foster, J. The Impact of Different Environmental Conditions on Cognitive Function: A Focused Review. *Front. Physiol.* **6** (2016).
6. Bateson, P. Genes, Environment and the Development of Behaviour. In *Novartis Foundation Symposium 213 - The Limits of Reductionism in Biology*, Novartis Foundation Symposia, 160–175, DOI: 10.1002/9780470515488.ch12 (2007).
7. Harel, Y., Nasser, R. A. & Stern, S. Mapping the developmental structure of stereotyped and individual-unique behavioral spaces in C. elegans. preprint, Neuroscience (2024). DOI: 10.1101/2024.01.27.577215.
8. Boogert, N. J., Madden, J. R., Morand-Ferron, J. & Thornton, A. Measuring and understanding individual differences in cognition. *Philos. Transactions Royal Soc. B: Biol. Sci.* **373**, 20170280, DOI: 10.1098/rstb.2017.0280 (2018). Publisher: Royal Society.
9. Kandel, E. R. & Hawkins, R. D. The Biological Basis of Learning and Individuality. *Sci. Am.* **267**, 78–87 (1992). Publisher: Scientific American, a division of Nature America, Inc.
10. Arican, C., Bulk, J., Deisig, N. & Nawrot, M. P. Cockroaches Show Individuality in Learning and Memory During Classical and Operant Conditioning. *Front. Physiol.* **10** (2020).
11. Kempermann, G. *et al.* The individuality paradigm: Automated longitudinal activity tracking of large cohorts of genetically identical mice in an enriched environment. *Neurobiol. Dis.* **175**, 105916, DOI: 10.1016/j.nbd.2022.105916 (2022).
12. Laskowski, K. L., Bierbach, D., Jolles, J. W., Doran, C. & Wolf, M. The emergence and development of behavioral individuality in clonal fish. *Nat. Commun.* **13**, 6419, DOI: 10.1038/s41467-022-34113-y (2022).
13. de Bivort, B. *et al.* Precise Quantification of Behavioral Individuality From 80 Million Decisions Across 183,000 Flies. *Front. Behav. Neurosci.* **16** (2022).
14. Spudich, J. L. & Koshland, D. E. Non-genetic individuality: chance in the single cell. *Nature* **262**, 467–471, DOI: 10.1038/262467a0 (1976).
15. Thomas F. Mathejczyk *et al.* Individuality across environmental context in Drosophila melanogaster. *bioRxiv* 2023.11.26.568741, DOI: 10.1101/2023.11.26.568741 (2023).
16. Xu, P. S., Lee, D. & Holy, T. E. Experience-Dependent Plasticity Drives Individual Differences in Pheromone-Sensing Neurons. *Neuron* **91**, 878–892, DOI: 10.1016/j.neuron.2016.07.034 (2016).
17. Finke, V., Baracchi, D., Giurfa, M., Scheiner, R. & Avarguès-Weber, A. Evidence of cognitive specialization in an insect: proficiency is maintained across elemental and higher-order visual learning but not between sensory modalities in honey bees. *J. Exp. Biol.* **224**, jeb242470, DOI: 10.1242/jeb.242470 (2021).
18. Ayroles, J. F. *et al.* Behavioral idiosyncrasy reveals genetic control of phenotypic variability. *Proc. Natl. Acad. Sci.* **112**, 6706–6711, DOI: 10.1073/pnas.1503830112 (2015). Publisher: Proceedings of the National Academy of Sciences.
19. Dudai, Y., Jan, Y. N., Byers, D., Quinn, W. G. & Benzer, S. dunce, a mutant of Drosophila deficient in learning. *Proc. Natl. Acad. Sci.* **73**, 1684–1688, DOI: 10.1073/pnas.73.5.1684 (1976). Publisher: Proceedings of the National Academy of Sciences.
20. Partridge, L. & Sgrò, C. M. Behavioural genetics: Molecular genetics meets feeding ecology. *Curr. Biol.* **8**, R23–R24, DOI: 10.1016/S0960-9822(98)70011-9 (1998). Publisher: Elsevier.
21. Koellinger, P. D. & Harden, K. P. Using nature to understand nurture. *Science* **359**, 386–387, DOI: 10.1126/science.aar6429 (2018). Publisher: American Association for the Advancement of Science.
22. Martin, G. M. Epigenetic drift in aging identical twins. *Proc. Natl. Acad. Sci.* **102**, 10413–10414, DOI: 10.1073/pnas.0504743102 (2005). Publisher: Proceedings of the National Academy of Sciences.

23. Honegger, K. & de Bivort, B. Stochasticity, individuality and behavior. *Curr. Biol.* **28**, R8–R12, DOI: 10.1016/j.cub.2017.11.058 (2018). Publisher: Elsevier.

24. Graham, J. H. Nature, Nurture, and Noise: Developmental Instability, Fluctuating Asymmetry, and the Causes of Phenotypic Variation. *Symmetry* **13**, DOI: 10.3390/sym13071204 (2021).

25. Buchanan, S. M., Kain, J. S. & de Bivort, B. L. Neuronal control of locomotor handedness in Drosophila. *Proc. Natl. Acad. Sci.* **112**, 6700–6705, DOI: 10.1073/pnas.1500804112 (2015). Publisher: Proceedings of the National Academy of Sciences.

26. Modi, M. N., Rajagopalan, A. E., Rouault, H., Aso, Y. & Turner, G. C. Flexible specificity of memory in Drosophila depends on a comparison between choices. *eLife* **12**, e80923, DOI: 10.7554/eLife.80923 (2023). Publisher: eLife Sciences Publications, Ltd.

27. Mollá-Albaladejo, R. & Sánchez-Alcañiz, J. A. Behavior Individuality: A Focus on Drosophila melanogaster. *Front. Physiol.* **12** (2021).

28. de Jong, H. L. Genetic Determinism: How Not to Interpret Behavioral Genetics. *Theory & Psychol.* **10**, 615–637, DOI: 10.1177/0959354300105003 (2000). Publisher: SAGE Publications Ltd.

29. Tosh, C. R. & Brogan, B. Environmental diversity constrains learning in Drosophila melanogaster. *Ecol. Entomol.* **42**, 697–703, DOI: 10.1111/een.12435 (2017). Publisher: John Wiley & Sons, Ltd.

30. Nepoux, V., Babin, A., Haag, C., Kawecki, T. J. & Le Rouzic, A. Quantitative genetics of learning ability and resistance to stress in Drosophila melanogaster. *Ecol. Evol.* **5**, 543–556, DOI: 10.1002/ece3.1379 (2015). Publisher: John Wiley & Sons, Ltd.

31. Williams-Simon, P. A. *et al.* Multiple genetic loci affect place learning and memory performance in Drosophila melanogaster. *Genes, Brain Behav.* **18**, e12581, DOI: 10.1111/gbb.12581 (2019). Publisher: John Wiley & Sons, Ltd.

32. Turner, C. H. *The homing of ants: an experimental study of ant behavior* (University of Chicago., 1907).

33. Turner, C. H. Experiments on pattern-vision of the honey bee. *The Biol. Bull.* **21**, 249–264 (1911). Publisher: Marine Biological Laboratory.

34. Smith, M. A.-Y., Honegger, K. S., Turner, G. & de Bivort, B. Idiosyncratic learning performance in flies. *Biol. Lett.* **18**, 20210424, DOI: 10.1098/rsbl.2021.0424 (2022). Publisher: Royal Society.

35. Álvarez Quintero, N. & Kim, S.-Y. Effects of maternal age and environmental enrichment on learning ability and brain size. *Behav. Ecol.* **35**, arae049, DOI: 10.1093/beheco/arae049 (2024).

36. Mao, W.-J., Wu, Z.-Y., Yang, Z.-H., Xu, Y.-W. & Wang, S.-Q. Advanced maternal age impairs spatial learning capacity in young adult mouse offspring. **10**, 975–988 (2018).

37. Luo, L. *et al.* Advanced Parental Age Impaired Fear Conditioning and Hippocampal LTD in Adult Female Rat Offspring. *Neurochem. Res.* **42**, 2869–2880, DOI: 10.1007/s11064-017-2306-9 (2017).

38. Mery, F. & Burns, J. G. Behavioural plasticity: an interaction between evolution and experience. *Evol. Ecol.* **24**, 571–583, DOI: 10.1007/s10682-009-9336-y (2010).

39. Chen, M. & Sokolowski, M. B. How Social Experience and Environment Impacts Behavioural Plasticity in Drosophila. *Fly* **16**, 68–84, DOI: 10.1080/19336934.2021.1989248 (2022). Publisher: Taylor & Francis.

40. Korner, A. F. Individual differences at birth: Implications for early experience and later development. *Am. J. Orthopsychiatry* **41**, 608–619, DOI: 10.1111/j.1939-0025.1971.tb03220.x (1971). Place: US Publisher: American Orthopsychiatric Association, Inc.

41. Beck, J., Ma, W., Pitkow, X., Latham, P. & Pouget, A. Not Noisy, Just Wrong: The Role of Suboptimal Inference in Behavioral Variability. *Neuron* **74**, 30–39, DOI: 10.1016/j.neuron.2012.03.016 (2012).

42. Hageter, J. *et al.* Environmental and Molecular Modulation of Motor Individuality in Larval Zebrafish. *Front. Behav. Neurosci.* **15** (2021).

43. Kawakami, K. *et al.* Exploring the genetic prediction of academic underachievement and overachievement. *npj Sci. Learn.* **9**, 39, DOI: 10.1038/s41539-024-00251-9 (2024).

44. Tully, T. & Quinn, W. G. Classical conditioning and retention in normal and mutantDrosophila melanogaster. *J. Comp. Physiol. A* **157**, 263–277, DOI: 10.1007/BF01350033 (1985).

45. Zhao, F., Zeng, Y., Guo, A., Su, H. & Xu, B. A neural algorithm for Drosophila linear and nonlinear decision-making. *Sci. Reports* **10**, 18660, DOI: 10.1038/s41598-020-75628-y (2020).

46. Yu, J. *et al.* Continuous, long-term crawling behavior characterized by a robotic transport system. .

47. Ofstad, T. A., Zuker, C. S. & Reiser, M. B. Visual place learning in Drosophila melanogaster. *Nature* **474**, 204–207, DOI: 10.1038/nature10131 (2011).

48. Mackay, T. F. C. *et al.* The Drosophila melanogaster Genetic Reference Panel. *Nature* **482**, 173–178, DOI: 10.1038/nature10811 (2012).

49. Alisch, T., Crall, J. D., Kao, A. B., Zucker, D. & de Bivort, B. L. MAPLE (modular automated platform for large-scale experiments), a robot for integrated organism-handling and phenotyping. *eLife* **7**, e37166, DOI: 10.7554/eLife.37166 (2018). Publisher: eLife Sciences Publications, Ltd.

50. Pickens, C. L. & Holland, P. C. Conditioning and cognition. *Neurobiol. Cogn. Lab. Animals: Challenges Oppor.* **28**, 651–661, DOI: 10.1016/j.neubiorev.2004.09.003 (2004).

51. Loesche, F. & Reiser, M. B. An Inexpensive, High-Precision, Modular Spherical Treadmill Setup Optimized for Drosophila Experiments. *Front. Behav. Neurosci.* **15** (2021).

52. Galsworthy, M. J. *et al.* Assessing Reliability, Heritability and General Cognitive Ability in a Battery of Cognitive Tasks for Laboratory Mice. *Behav. Genet.* **35**, 675–692, DOI: 10.1007/s10519-005-3423-9 (2005).

53. Chittka, L., Giurfa, M. & Riffell, J. A. Editorial: The Mechanisms of Insect Cognition. *Front. Psychol.* **10** (2019).

54. Nouvian, M. & Galizia, C. G. Aversive Training of Honey Bees in an Automated Y-Maze. *Front. Physiol.* **10** (2019).

55. Bengochea, M. *et al.* Numerical discrimination in Drosophila melanogaster. *Cell Reports* **42**, DOI: 10.1016/j.celrep.2023.112772 (2023). Publisher: Elsevier.

56. Giurfa, M., Zhang, S., Jenett, A., Menzel, R. & Srinivasan, M. V. The concepts of 'sameness' and 'difference' in an insect. *Nature* **410**, 930–933, DOI: 10.1038/35073582 (2001).

57. Savall, J., Ho, E. T. W., Huang, C., Maxey, J. R. & Schnitzer, M. J. Dexterous robotic manipulation of alert adult Drosophila for high-content experimentation. *Nat. Methods* **12**, 657–660, DOI: 10.1038/nmeth.3410 (2015).

58. Croteau-Chonka, E. C. *et al.* High-throughput automated methods for classical and operant conditioning of Drosophila larvae. *eLife* **11**, e70015, DOI: 10.7554/eLife.70015 (2022). Publisher: eLife Sciences Publications, Ltd.

59. Gong, Z.-F., Xia, S.-Z., Liu, L., Feng, C.-H. & Guo, A.-K. Operant visual learning and memory in Drosophila mutants dunce, amnesiac and radish. *J. Insect Physiol.* **44**, 1149–1158, DOI: 10.1016/S0022-1910(98)00076-6 (1998).

60. Harris, W. A. & Stark, W. S. Hereditary retinal degeneration in Drosophila melanogaster. A mutant defect associated with the phototransduction process. *J. Gen. Physiol.* **69**, 261–291, DOI: 10.1085/jgp.69.3.261 (1977).

61. Anderson, C. *et al.* Natural variation in stochastic photoreceptor specification and color preference in Drosophila. *eLife* **6**, e29593, DOI: 10.7554/eLife.29593 (2017). Publisher: eLife Sciences Publications, Ltd.

62. Van Dongen, S. & Møller, A. P. On the distribution of developmental errors: comparing the normal, gamma, and log-normal distribution. *Biol. J. Linnean Soc.* **92**, 197–210, DOI: 10.1111/j.1095-8312.2007.00880.x (2007).

63. Klingenberg, C. P. Phenotypic Plasticity, Developmental Instability, and Robustness: The Concepts and How They Are Connected. *Front. Ecol. Evol.* **7** (2019).

64. Garrido-Jurado, S., Muñoz-Salinas, R., Madrid-Cuevas, F. & Marín-Jiménez, M. Automatic generation and detection of highly reliable fiducial markers under occlusion. *Pattern Recognit.* **47**, 2280–2292, DOI: 10.1016/j.patcog.2014.01.005 (2014).

65. Ernesto Salcedo *et al.* Blue- and Green-Absorbing Visual Pigments ofDrosophila: Ectopic Expression and Physiological Characterization of the R8 Photoreceptor Cell-Specific Rh5 and Rh6 Rhodopsins. *The J. Neurosci.* **19**, 10716, DOI: 10.1523/JNEUROSCI.19-24-10716.1999 (1999).

66. Schnaitmann, C., Garbers, C., Wachtler, T. & Tanimoto, H. Color Discrimination with Broadband Photoreceptors. *Curr. Biol.* **23**, 2375–2382, DOI: 10.1016/j.cub.2013.10.037 (2013).

67. Whishaw, I. Q. Place Learning in Hippocampal Rats and the Path Integration Hypothesis. *Neurosci. & Biobehav. Rev.* **22**, 209–220, DOI: 10.1016/S0149-7634(97)00002-X (1998).

68. Melnattur, K. V. *et al.* Multiple Redundant Medulla Projection Neurons Mediate Color Vision in Drosophila. *J. Neurogenetics* **28**, 374–388, DOI: 10.3109/01677063.2014.891590 (2014). Publisher: Taylor & Francis.

69. Frossard, J. & Renaud, O. Permutation Tests for Regression, ANOVA, and Comparison of Signals: The permuco Package. *J. Stat. Softw.* **99**, 1 – 32, DOI: 10.18637/jss.v099.i15 (2021). Section: Articles.

70. Strasser, H. & Weber, C. *On the asymptotic theory of permutation statistics*. Report (Vienna University of Economics and Business Administration, 1999).

71. Hothorn, T., Hornik, K., van de Wiel, M. A. & Zeileis, A. Implementing a Class of Permutation Tests: The coin Package. *J. Stat. Softw.* **28**, 1 – 23, DOI: 10.18637/jss.v028.i08 (2008). Section: Articles.

72. Cover, T. M. & Thomas, J. A. *Elements of Information Theory* (John Wiley & Sons, Inc., Hoboken, New Jersey., 2006), 2 edn.

73. Hellinger, E. Neue Begründung der Theorie quadratischer Formen von unendlichvielen Veränderlichen. **1909**, 210–271, DOI: 10.1515/crll.1909.136.210 (1909).

74. Shannon, C. E. A Mathematical Theory of Communication. *Bell Syst. Tech. J.* **27**, 379–423, DOI: 10.1002/j.1538-7305.1948.tb01338.x (1948). Publisher: John Wiley & Sons, Ltd.

75. Hausser, J. & Strimmer, K. Entropy Inference and the James-Stein Estimator, With Application to Nonlinear Gene Association Networks. *J. Mach. Learn. Res.* **10**, DOI: 10.1145/1577069.1755833 (2008).

76. Kullback, S. & Leibler, R. A. On Information and Sufficiency. *The Annals Math. Stat.* **22**, 79–86 (1951). Publisher: Institute of Mathematical Statistics.

77. Drost, H.-G. Philentropy: Information Theory and Distance Quantification with R. *J. Open Source Softw.* **3**, 765, DOI: 10.21105/joss.00765 (2018).

78. Huys, Q. J. M. *et al.* Bonsai trees in your head: How the pavlovian system sculpts goal-directed choices by pruning decision trees. *PLoS Comput. Biol.* **8**, e1002410, DOI: 10.1371/journal.pcbi.1002410 (2012).

Acknowledgements

We would like to thank Samuel Bourgeat for helpful discussions and help with fly care, Wulfram Gerstner for the compute time on the cluster, the PCB Lab at the EPFL's School of Engineering, for providing equipment and material for the fabrication of printed circuit boards used in the project, and the members of the "Project Flybot" WhatsApp chat group (Tomislav Štampar, Stjepan Bukal, Marko Jakšić and Samuel Bourgeat) for the moral and technical support during design of the platform. This study was funded by EPFL School of Life Science ELISIR scholarship.

Additional information

Competing interests All authors declare no competing interest.
GitHub code repository https://github.com/jaksiclab/GeneticsOfLearningIndividuality
Author contributions AMJ and RM conceptualized and designed the study. RM, AMJ and IT conceptualized and designed the behavior platform. RM built the platform's software, RM and AMJ built the experimental hardware. RM, GVB and AMJ performed the experiments. RM, JB, AMJ and AM conceptualized the data analysis. RM, JB, GVB and AMJ analyzed the data and produced the results. AMJ, RM and JB wrote the manuscript. All authors read, edited and intellectually significantly contributed to the manuscript.